BRAIN: ANATOMICAL CONNECTIVITY FOR EFFECTIVE CONNECTIVITY OPTIMIZATION

René Labounek

Doctoral Degree Programme (2), FEEC BUT

E-mail: xlabou01@stud.feec.vutbr.cz

Supervised by: Jiří Jan

E-mail: jan@feec.vutbr.cz

Abstract: The study deals with optimization of effective brain connectivity with prior knowledge based on anatomical connectivity. Main attention is dedicated to distributions of anatomical connectivity probabilities over population of examined subjects between regions of interest selected on the basis of fMRI activation maps with motor task. Closing part describes how parameters of distributions should affect effective connectivity estimation.

Keywords: anatomical and effective connectivity, fMRI, diffusion MRI, dynamic causal modelling

1. INTRODUCTION

Via MR scanner, it is possible to reconstruct white matter tracts and indirectly measure gray matter activity. For white matter tracts reconstruction, there are used gradient-based sequences sensitive at water diffusion motion (diffusion MRI, dMRI). Anisotropic water diffusion over 3D space is characteristic for parts of brain where white matter is [1]. Firstly, water diffusion decomposition is estimated per each voxel and then the white matter tracts are reconstructed via tractography on decomposed dMRI data [2]. The system of white matter tracts is called anatomical connectivity. The example of anatomical connectivity you can see in Figure 1a.

Functional magnetic resonance imaging (fMRI) is a method of indirect measuring of brain activity in gray matter which evokes hemodynamic changes. The changes are described with hemodynamic model [3] where concentration change of paramagnetic deoxy-hemoglobin (deoxy-Hb) figures. Deoxy-Hb concentration change increases inhomogeneity of stationary homogeneous magnetic field and decreases T_2* relaxation time. With repetitive scanning, it is possible to measure temporal changes of T_2* relaxation time called BOLD signal (blood oxygen level dependence), last state value of hemodynamic model [4]. The neuronal activity can be reconstructed with inversion of hemodynamic model.

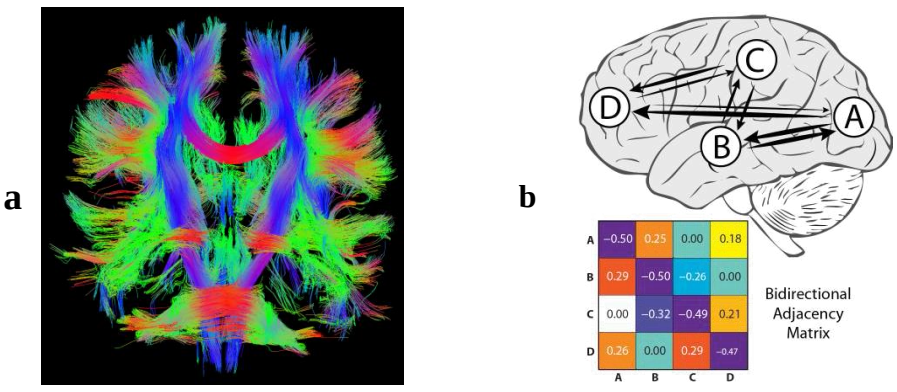

Figure 1: Anatomical (a) and effective (b) connectivity [5], [6]

The general linear model approach is most commonly used for founding of activated parts of brain [7]. If you have found activated brain areas you can analyze causality between those areas with dynamic causal modelling (DCM) which uses hemodynamic model inversion [8]. The DCM output is bidirectional matrix of effective connectivity. The example of effective connectivity you can see in Figure 1b.

Because DCM is based on prior-posterior Bayesian estimation approach, Stephan et al. introduced a pilot study how the anatomical connectivity informed priors could improve posterior DCM knowledge in 2009 [9]. They designed 62 different models where prior variance was influenced by probability of anatomical connection and showed that for some parameter settings of variance calculation, the final posterior DCM models has higher log-evidence [10] than for model without anatomical connectivity. But their methodology has several limitations they have not used dMRI and fMRI data measured on same subjects and did not use this optimization for fully-connected model where tractography-based priors could have greater application.

For this reason, we tried to replicate their approach for the dMRI-fMRI dataset measured on same subjects (11 persons) with motor task during fMRI experiment and used fully-connected model. The results showed that some anatomical-connectivity based models has higher log-evidence over priors commonly used in 2009 but not over priors used now [11]. Because the standard deviations of anatomical connection probabilities between regions of interest (ROIs) were predominantly in the same orders as the probability itself we recalculate anatomical connectivity probabilities for 37 persons and the results are described below.

2. METHODOLOGY

2.1. DATA

Open-access preprocessed dMRI-fMRI dataset from the database humanconnectome.org was used [12], [13]. Data are on experimental high level quality because dMRI data were acquired from 270 gradient directions with 1.25mm isotropic voxels (168x144x111), field of view (FOV) 210*180mm, multi-shell scanning protocol (b-values: 1000, 2000 and 3000 s/mm^2) and fMRI data were acquired in spatial-temporal resolution 2mm isotropic voxels (104x90x72) with repetition time of scanning TR=720ms, FOV 208x180mm. Motor task during fMRI acquisition was divided on 2 independent runs (sessions), each containing 284 fMRI scans (run duration 3 min 34 s).

2.2. FMRI MOTOR TASK PROTOCOL

Participants are presented with visual cues that ask them to either tap their left or right fingers, or squeeze their left or right toes, or move their tongue to map motor areas. Each block of a movement type lasted 12 seconds (10 movements), and is preceded by a 3 second cue. In each of the two runs, there are 13 blocks, with 2 of tongue movements, 4 of hand movements (2 right and 2 left), and 4 of foot movements (2 right and 2 left). In addition, there are 3 15-second fixation blocks per run [12], [14].

2.3. WATER DIFFUSION DECOMPOSITION

Water diffusion was decomposed from dMRI data into 3 partial directions per voxel with ball and stick model optimized for multi-shell scanning protocol with Rician noise in the data [15] implemented in *FSL* software library [16]. The outputs of decomposition are inputs for probabilistic tractography [2].

2.4. FMRI-BASED PROBABILISTIC TRACTOGRAPHY

Based on general linear model approach implemented in software *Statistical Parametric Mapping 8 (SPM8, Welcome Trust Centre, London)* and 2nd level group statistic on data from 37 subjects, 6 ROIs where the supra-thresholded activity was observable during left (L) or right (R) hand move-

ment have been selected. It was: 2 primary motor cortices L Brodman Area 3 (LBA3) and RBA4; 2 secondary motor cortices LBA6 (or LSMA – supplementary motor area) and RBA6 (or RSMA); and 2 activated parts of cerebellum L Culmen and R Culmen. The results were in standardized MNI space (Montreal Neurological Institute coordinates).

Nearby those activated clusters in white matter, masks (seeds and targets) for probabilistic tractography were manually created in MNI space and then transformed with *FSL* software [16] into diffusion space of each subject.

Masks in diffusion space of each subject were used as seeds and targets for all combinations of anatomical connections between ROIs (6 ROIs → 15 combinations of direct anatomical connections). For each voxel in a seed mask, 20 000 tracks were traced. In target, there was calculated how many tracks got into target, when it happened the tracking of this track was ended. For each anatomical connection, double tracking was calculated, firstly one mask was a seed and second one a target and secondly it was conversely. The probability of each direct anatomical connection was then calculated according to equation (1) because dMRI data are unidirectional.

$$P_{AB} = \frac{T_A + T_B}{S_A + S_B} \tag{1}$$

P_{AB} is a probability of anatomical connection between ROIs A and B. T_A and T_B are number of traces which got into target A or B. S_A and S_B are number of traces traced from seed A or B.

The probabilities were then transformed on relative probabilities (2) as in Stephan et al. study [9].

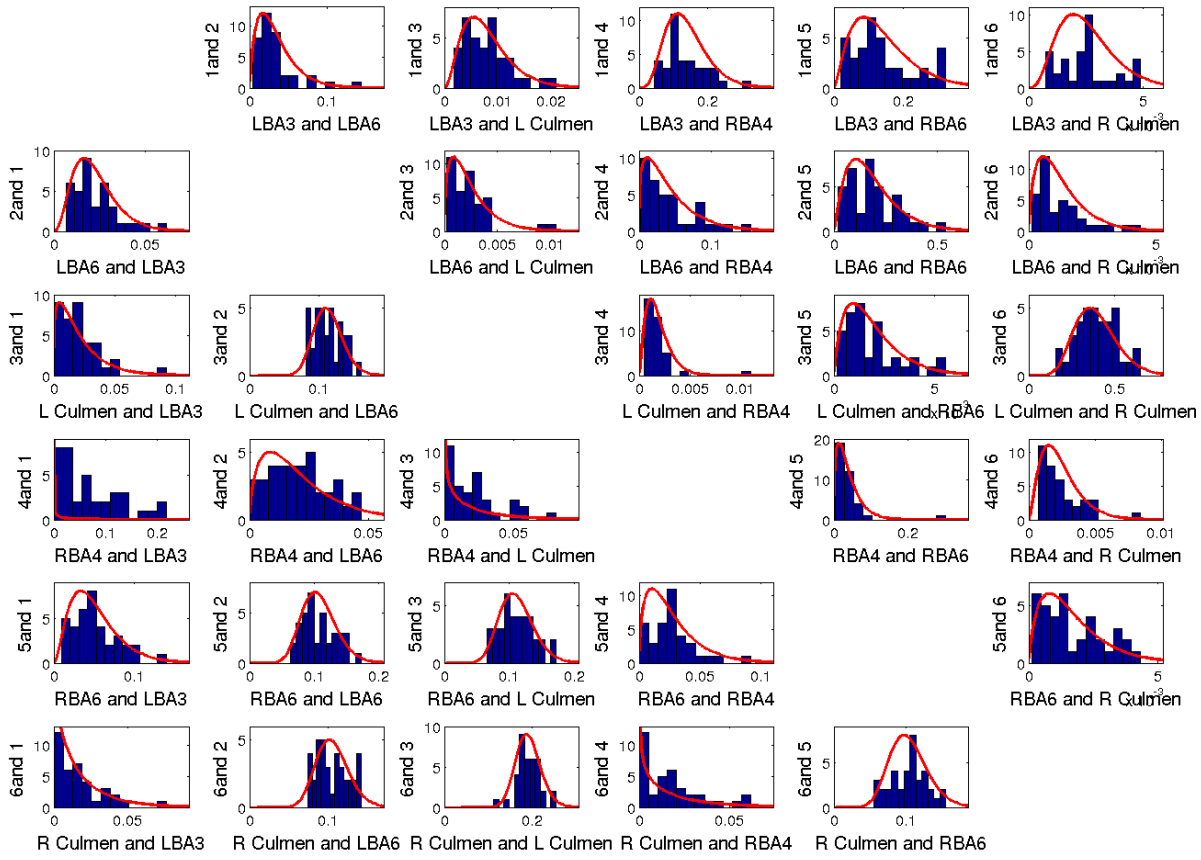

Figure 2: Distributions of relative probability of anatomical connection between ROIs; x-axis is relative probability of anatomical connection, y-axis is number of subject with probability on a given interval; right part is for 1st level tracking, left part for 2nd level tracking; the red curves show estimated gamma distributions.

$$\delta P_{ABi} = \frac{P_{ABi}}{\sum_{i=1}^{15} P_{ABi}} \tag{2}$$

Because the precision of tractography is low nearby gray matter, 2nd level tractography was estimated. Seed for tracking between A and B was placed into location where at least 5% of traces went through from seeds A or B during previous tractographies. The final probability was then calculated as probability of two independent probabilities according to equation 3 and transformed into relative probability according to equation 2.

$$P_{AB} = P_A P_B = \frac{T_A T_B}{S_{5\%}^2} \tag{3}$$

In this study, the area of interest was if larger subject sample (37 now; 11 before) decreases the orders of probability standard deviations when classical average is used and if the distributions of anatomical connectivity probabilities between ROIs are normally distributed or not. This knowledge is necessary for precise design of prior information for effective connectivity estimation.

3. RESULTS

The orders of standard deviations were not decreased when classical average was used. As you can see in Figure 2 all distributions of relative probabilities of anatomical connectivity are not normally distributed but gamma distributed for both 1st level and 2nd level tracking.

When the parameters of gamma distributions were estimated and the averages were replaced with mean values of gamma distribution, the orders of variances and standard deviations decreased. It shows that the gamma distribution characterizes this data better than the normal distribution.

2nd level tracking disposes with „eliminating" property of some anatomical connections. In left part of Figure 2, the probability density functions (PDFs, red curves) whose shape is a part of hyperbole indicate that it is the most probable that there is not any direct anatomical connection.

4. CONCLUSIONS

The standard deviations were not decreased when average was used because distributions of relative probabilities of anatomical connection between ROIs are gamma distributed.

It seems that results of 2nd level tracking are more in line with reality because it eliminated probability of direct anatomical connection between primary motor cortices and parts of cerebellum on almost zero. It means that cerebellum communicates more probably only with secondary motor cortices and between themselves. Moreover 1st level tracking disposes with high relative probability for anatomical connection between L and R Culmen which is more probably an artifact than real situation. The artifact is probably caused by cerebellum shape.

In next process of effective connectivity optimization: It is possible that mean value of gamma distribution for determining of prior variance in DCM estimation could be more powerful than average used before [9], [11]. We will also try to use the „eliminating" property. If PDF shape will be a hyperbole, the prior knowledge will be that there is not any linkage. It could be able to generate anatomical informed prior models of effective connectivity. DCM limitation is that it cannot generate the best model but only choose the best one from the set of input models.

ACKNOWLEDGEMENT

The research was supported by Grant Agency of Czech Republic by the grant no. P103/12/0552. The funding is highly acknowledged.

Data were provided [in part] by the Human Connectome Project, WU-Minn Consortium (Principal Investigators: David Van Essen and Kamil Ugurbil; 1U54MH091657) funded by the 16 NIH Insti-

tutes and Centers that support the NIH Blueprint for Neuroscience Research; and by the McDonnell Center for Systems Neuroscience at Washington University.

Access to computing and storage facilities owned by parties and projects contributing to the National Grid Infrastructure MetaCentrum, provided under the programme "Projects of Large Infrastructure for Research, Development, and Innovations" (LM2010005), is greatly appreciated.

Access to the CERIT-SC computing and storage facilities provided under the programme Center CERIT Scientific Cloud, part of the Operational Program Research and Development for Innovations, reg. no. CZ. 1.05/3.2.00/08.0144, is greatly appreciated.

REFERENCES

[1] P. J. Basser, J. Mattiello, and D. LeBihan, "MR diffusion tensor spectroscopy and imaging," *Biophys. J.*, vol. 66, no. 1, pp. 259–67, Jan. 1994.

[2] T. E. J. Behrens, H. J. Berg, et al., "Probabilistic diffusion tractography with multiple fibre orientations: What can we gain?," *Neuroimage*, vol. 34, no. 1, pp. 144–55, Jan. 2007.

[3] R. B. Buxton, E. C. Wong, and L. R. Frank, "Dynamics of blood flow and oxygenation changes during brain activation: the balloon model.," *Magn. Reson. Med.*, vol. 39, no. 6, pp. 855–64, Jun. 1998.

[4] S. Ogawa, T. M. Lee, et al., "Brain magnetic resonance imaging with contrast dependent on blood oxygenation.," *Proc. Natl. Acad. Sci. U. S. A.*, vol. 87, no. 24, pp. 9868–72, Dec. 1990.

[5] G. Williams, "UAB Research," 2013. [Online]. Available: http://themixuab.blogspot.cz/2013/04/image-post-1-brain-message-superhighways.html.

[6] M. Havlíček and J. Jan, "Exploring brain network connectivity through hemodynamic modeling," Brno University of Technology, 2011.

[7] K. J. Friston, A. P. Holmes, et al., "Statistical Parametric Maps in Functional Imaging : A General Linear Approach," *Hum. Brain Mapp.*, vol. 2, no. 4, pp. 189–210, 1995.

[8] K. J. Friston, L. Harrison, and W. Penny, "Dynamic causal modelling," *Neuroimage*, vol. 19, no. 4, pp. 1273–1302, Aug. 2003.

[9] K. E. Stephan, M. Tittgemeyer, et al., "Tractography-based priors for dynamic causal models.," *Neuroimage*, vol. 47, no. 4, pp. 1628–38, Oct. 2009.

[10] K. E. Stephan, W. D. Penny, et al., "Bayesian model selection for group studies.," *Neuroimage*, vol. 46, no. 4, pp. 1004–17, 2009.

[11] R. Labounek, M. Gajdoš, et al., "Sigmoid function parameter stability in anatomically informed priors for dynamic causal models," in *OHBM*, 2014, pp. 1–2.

[12] D. C. Van Essen, K. Ugurbil, et al., "The Human Connectome Project: a data acquisition perspective.," *Neuroimage*, vol. 62, no. 4, pp. 2222–31, Oct. 2012.

[13] M. F. Glasser, S. N. Sotiropoulos, et al., "The minimal preprocessing pipelines for the Human Connectome Project.," *Neuroimage*, vol. 80, pp. 105–24, Oct. 2013.

[14] R. L. Buckner, F. M. Krienen, et al., "The organization of the human cerebellum estimated by intrinsic functional connectivity," vol. 02138, pp. 2322–2345, 2011.

[15] S. Jbabdi, S. N. Sotiropoulos, et al., "Model-based analysis of multishell diffusion MR data for tractography: how to get over fitting problems.," *Magn. Reson. Med.*, vol. 68, no. 6, pp. 1846–55, Dec. 2012.

[16] M. Jenkinson, C. F. Beckmann, et al., "Fsl.," *Neuroimage*, vol. 62, no. 2, pp. 782–90, Aug. 2012.